5-1-2021

On Compressional Wave Attenuation in Muddy Marine Sediments

Charles W. Holland
Portland State University, hollan7@pdx.edu

Stan E. Dosso
University of Victoria

Citation Details

Holland, C. W., & Dosso, S. E. (2021). On compressional wave attenuation in muddy marine sediments. *The Journal of the Acoustical Society of America*, *149*(5), 3674–3687. https://doi.org/10.1121/10.0005003

On compressional wave attenuation in muddy marine sediments

Charles W. Holland[1] and Stan E. Dosso[2]

[1] Portland State University, Portland, Oregon, USA, email: charles.holland@pdx.edu
[2] University of Victoria, Victoria, British Columbia, Canada

Abbreviated title: Attenuation in muddy sediments
Date uploaded to JASA manuscript submission system: 4 January 2021
Revision uploaded to JASA manuscript submission system: 23 March 2021

Abstract

A method for measuring *in-situ* compressional wave attenuation exploiting the spectral decay of reflection coefficient Bragg resonances is applied to fine-grained sediments in the New England Mud Patch. Measurements of layer-averaged attenuation in a 10.3 m mud layer yield 0.04 {0.03 0.055} dB/m/kHz (braces indicate outer bounds); the attenuation is twice as large at a site with 3.2 m mud thickness. It is shown that both results are heavily influenced by a ~1 m sand-mud transition interval created by geological and biological processes which mix sand (at the base of the mud) into the mud. Informed by the observations, it appears that the spatial dependence of mud layer attenuation across the New England Mud Patch can be predicted by accounting for the transition interval via simple scaling. Further, the ubiquity of the processes that form the transition interval suggests that the scaling may be applied to any muddy continental shelf. In principle, attenuation predictions in littoral environments could be substantively improved with a modest amount of geologic and biologic information.

I. INTRODUCTION

Sediment compressional wave attenuation is one of the most important quantities needed for accurate prediction of waveguide (long-range) propagation and reverberation in bottom-limited ocean environments inasmuch as it largely controls losses below the critical angle. This applies to both sandy and muddy sediments, but even more so to the latter, where the waveguide includes the mud layer (due to the sound speed generally being less than that of the water). In other words, in long-range propagation, acoustic/seismic waves propagate through the mud layer, whereas in sandy sediments the field decays exponentially.

Though clearly an important quantity, attenuation is also one of the most difficult geoacoustic properties to measure and uncertainties tend to be large, especially at frequencies in the kilohertz regime and below. Part of the difficulty is that path length (in terms of wavelengths) needs to be sufficiently large through the sediment so that attenuation is detectable and separable from other loss mechanisms. This can be attempted from a core sample at hundreds of kilohertz; however, at these frequencies shell fragments and sand grains found in natural marine sediments cause scattering that substantively increase the attenuation. The scattering losses are essentially impossible to account for, at least to date. At low frequencies, the long path lengths required make it challenging to separate out attenuation in a specific layer; sandy and muddy layers often cannot be separated either because lack of knowledge of their grain size distribution or inability to control dominant acoustic paths. Muddy sediments can exhibit an attenuation that is 1 to 2 orders of magnitude smaller than that in sand and this further increases the difficulty.

One of the earliest measurements of *in-situ* marine mud attenuation was performed in the 1960s by Wood and Weston [1] in a harbor with 1 m of mud overlying gravel. It is notable that the first *in-situ* measurement attempt was unsuccessful because the laboratory attenuation measurements (from cores of the same harbor mud) were far too high, which led to improper data acquisition settings. A subsequent successful *in-situ* attempt resulted in attenuation with a value of 0.066 dB/m/kHz that scaled linearly with frequency from 2-48 kHz. A decade later, Hamilton [2] published a large compilation of *in-situ* and laboratory data from a variety of sediments, concluding that attenuation varied approximately linearly with frequency. He also developed regression relations based on porosity or mean grain size. Fine-grained, or muddy, sediments range in porosity roughly from 60 – 90% and his empirical relations vary by nearly one order of magnitude over that range, 0.4 – 0.05 dB/m/kHz. Some time later, Hamilton [3] suggested, from rather sparse data, that fine-grained sediment attenuation increases with increasing depth in the sediment, with a (positive) gradient of 3×10^{-4} dB/m^2/kHz in the upper few hundred meters of sediment.

Several decades later, Bowles [4] recognized that Hamilton's empirical relations did not predict fine-grained (muddy) sediment attenuation accurately. Bowles made a new data compilation by filtering Hamilton's data [2] based on sediment texture, limiting the new data compilation to include only fine-grained sediments and adding newer measurements. From the new compilation Bowles concluded 1) that attenuation follows a linear or nearly linear frequency dependence (in agreement with Hamilton), 2) that Hamilton's attenuation for fine-grained sediments is about one order of magnitude too high, and 3) that Hamilton's depth-dependent attenuation profile needed refinement. Bowles concluded that attenuation and its depth-dependence could be bracketed by two profiles from Mitchell and Focke [5]. These profiles have near-surface attenuation values of 0.004 and 0.026 dB/m/kHz and positive gradients in the upper few hundred meters of sediment

(4×10^{-5} and 8×10^{-5} dB/m^2/kHz at the water-sediment interface). The Mitchell-Focke curves were estimated in deep water turbidite regimes, i.e., fine-grained sediment with intercalating silt and sand layers, indicating that even the 0.004 dB/m/kHz value may be biased high compared to 'pure' mud.

It is appropriate to point out that the term 'mud' encompasses a wide range of sediments, from sediments whose dominant component is silt with a non-negligible sand component (as in this study), to sediments dominated by clay with some silt and nearly negligible sand fraction (as in [6]). This is to say that muddy sediments have a wide range of geological, geophysical, and geoacoustical properties. Thus, while the two Mitchell-Focke curves may be useful as bounds, Bowles unfortunately did not provide a way to estimate attenuation based on, say, porosity or mean grain size over that wide range. Moreover, there is some contradiction in his results. His improved compilation of fine-grained attenuation measurements are fit by a frequency dependence of $2.42 \times 10^{-5} f^{1.12}$ (dB/m) [4]. However, in apparent contradiction to his conclusions, this fit yields values considerably higher than the upper bound of the surficial Mitchell-Focke curves, e.g., 0.05 dB/m/kHz at 500 Hz. This would seem to imply that Bowles' compilation, while an improvement from Hamilton, still has considerable bias from the presence of measurement artifacts, including embedded sands.

One question not raised or addressed by Bowles is whether fine-grained sediment attenuation is expected to be similar in shallow- and deep-water environments. Bowles' [4] recommended curves (Mitchell-Focke) were solely derived from deep-water environments. There are several reasons why shallow-water fine-grained sediments could exhibit different attenuation. In coastal regions, the terrigenous component of fine-grained sediments may be expected to be higher; also the smallest grain sizes (micron scale) tend to move onto the slope or abyssal regions. In addition, deposition rates are considerably higher in shallow than in deep water; this likely affects compaction, and hence depth dependence, of attenuation. Sea-level oscillations and coastal ocean dynamics play major roles in mud distribution in shallow water, and limit mud thickness in shallow water to a few tens of meters, whereas in deep-water environments, mud thicknesses are commonly many kilometers. However, since the dominant mechanism(s) in fine-grained sediments that control attenuation are as yet only speculative, it is not clear whether these factors suggest that fine-grained sediment attenuation should differ between deep- and shallow-water settings.

In order to briefly address this question, two shallow-water measurements made subsequent to Bowles work are noted. In the late 1990s, attenuation measurements were made in fine-grained sediments off the Eel River shelf [7] using an Acoustic Lance [8] operating at 7.5 kHz. The relevant conclusions are that

- At all sites there was strong decrease in attenuation in the upper meter of sediment, i.e., a *negative* attenuation gradient. The ratio between the attenuation at the seafloor and 1 m below was as much as a factor of 4. This is significant, because it is contrary to what Hamilton and then Bowles concluded. The latter recommended the two Mitchell-Focke curves, which exhibit a positive attenuation gradient [4] in the upper few hundred meters. It should be noted (though Bowles did not refer to it) that Mitchell and Focke [5] Fig. 11 show a third result where the attenuation decreases over the upper 150 m in depth which they label 'medium attenuation' as opposed to 'low' or 'high attenuation'. It is also important to note the vastly different depth scales; the Eel River delta measurements

focus on the upper 2 m of sediments with ~ 0.3 m resolution, whereas Mitchell and Focke's resolution is considerably lower, ~10 m near the water-sediment interface.

- At 4 out of 6 sites, *in-situ* attenuation (7.5 kHz) was of order 0.01 dB/m/kHz below 1 m sub-bottom.
- At 2 out of 6 sites, *in-situ* attenuation (7.5 kHz) was of order 0.1 dB/m/kHz below 1 m sub-bottom. It is not clear why the attenuations at a few locations were so much higher, whether shell fragments and/or large grains played a role, or whether it was due to the significant heterogeneity from biologic processes and flooding events noted in the study.
- Co-located *in-situ* and laboratory measurements were made at numerous sites. The laboratory attenuation (measured on cores) was generally far higher, sometimes an order of magnitude, than the *in-situ* measurements.

Another shallow-water measurement [6] at lower frequencies, 1-3.6 kHz, yielded a mud layer-averaged attenuation of 0.009 [0.006, 0.013] dB/m/kHz (mean and 95% credibility interval from Bayesian reverberation inversion), where the averaging depth was over a 10 m thick mud layer in 100 m water depth on the Malta Plateau (south of Sicily). The Eel River delta and Malta Plateau results provide evidence that shallow-water mud attenuation can be of order 0.01 dB/m/kHz, i.e. comparable to those in deep water.

In summary, laboratory measurements of attenuation (at hundreds of kilohertz) from cores give values that are not suitable for extrapolating to lower frequencies. Though *in-situ* methods seem to have promise and some measurements are beginning to shed light on attenuation in shallow-water fine-grained sediments, *in-situ* measurement techniques are still in relatively early development and there is a paucity of data particularly in shallow-water environments at hundreds to thousands of hertz. The focused objective of this research is to measure the frequency-dependent attenuation of the mud layer on the New England Mud Patch (NEMP). This is part of our long-term science objective to measure the intrinsic frequency dependence of the sound speed and attenuation in muddy sediments from a few hundred hertz to a few kilohertz (see [9]) and closely connected to the broad goals of the ONR-supported Seabed Characterization Experiment, see [10].

Our findings at the NEMP indicate that an interval at the base of the mud, the sand-mud transition interval, has a high attenuation which strongly affects the mud layer-averaged attenuation. This transition interval turns out to be crucial to understanding the spatial variability of the mud layer-averaged attenuation at the NEMP. More broadly, we have reasoned that since the transition interval is created by biologic and geologic processes that operate in virtually all muddy continental shelf regions, the transition interval must also exist in all muddy continental shelf regions. The implication of this is that key characteristics of depth-dependent and layer-averaged attenuation may be predictable in muddy shelf environments around the world. Both the findings at the NEMP and of data outside the NEMP are considered to explore this conjecture.

Section II of this paper presents current understanding of the mud layer at the NEMP and proposes a subdivision into geoacoustic-based intervals. Section III contains the main body of results, presenting a new approach to measuring attenuation which exploits the decay of the Bragg interference pattern at low grazing angles, and compares attenuation results with other methods at the same site and other locations within the NEMP. Attenuation data outside the

NEMP are also presented along with a first look at the existence of the sand-mud transition interval and its characteristics elsewhere. Section IV provides additional discussion on key findings including the likely global role of the transition interval. A summary is given in Section V.

II. MUD LAYER STRUCTURE AND CHARACTERISTICS

An overview of the mud structure at the NEMP is given in this section drawing on a chirp sub-bottom profiling survey [11], extensive coring [12], and wide-angle reflection coefficient inversions [13]. The experiment area is shown in Figure 1 along with the position of the two reflection coefficient sites discussed here: SWAMI, a thick mud (10.3 m) location near the center of the area; and VC31-2, a thin mud (3.2 m) location near its western edge. The SWAMI site location, 70.5753 W 40.4614 N is named for its proximity to the SWAMI array, which is ~1 km ESE. The VC31-2 site, 70.7469 W 40.4838 N, is named from the nearby core designation. The two sites are 14.8 km apart. Detailed information on the design of these experiments are given in [9].

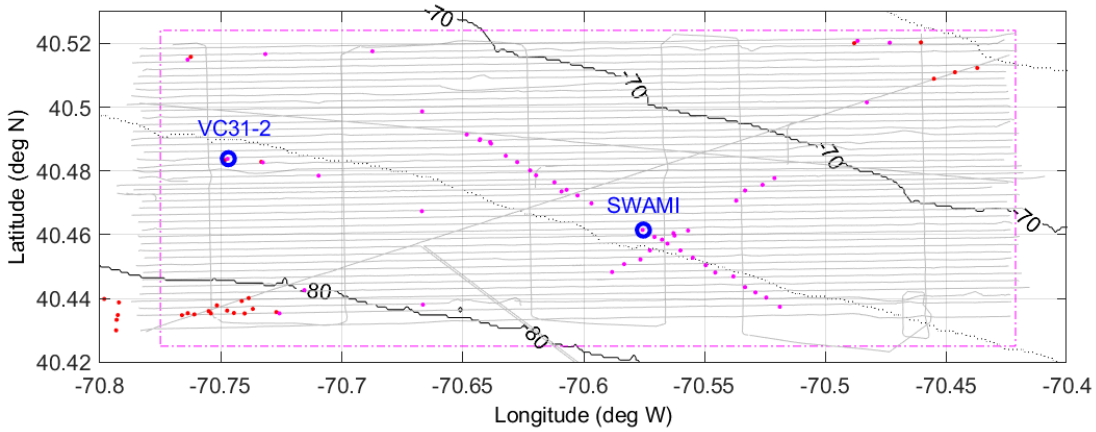

Figure 1. *Map of experiment area in the New England Mud Patch showing bathymetry (m) and the two wide-angle reflection sites (o) where attenuation is estimated. Core locations (dots) and sub-bottom profiling lines (gray) are also shown. (Color online)*

A. Sub-bottom profiling data

Extensive sub-bottom profiling data (0.5-7.2 kHz) were collected in the NEMP and the time domain data were analyzed to produce reflecting horizon isopach maps, Goff et al. [11]. Mud thickness varies from about 3-12 m across the experiment area, with the thickest mud in the central area. A total of 5 reflecting horizons were mapped in the mud layer; from bottom to top these are termed mh1 through mh5 (following the direction of geologic time). The horizon below mh1 is termed the mudbase (mb) and above mh5 is the water-sediment interface. The mud reflecting horizons (mh) can arise from a step impedance change (Figure 2a) or a thin layer sandwiched between virtually identical layers (Figure 2b). This latter impedance profile is not uncommon in muddy sediments where a thin sand intercalating layer can be deposited by a single climatic event superposed on an otherwise approximately constant depositional environment. When the intercalating layer thickness, h, is small enough (less than 0.2 m) that the seismic pulse cannot resolve the top and bottom of the layer, the reflected arrival appears as a

single horizon so that it is not possible to determine which profile caused the reflection, Figure 2a or b. Thus, the five mud horizons individually could represent Figure 2a or Figure 2b.

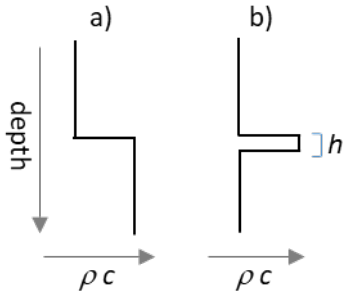

Figure 2. *Cartoon of possible vertical impedance profiles sensed by sub-bottom profiler data: a) step function impedance change, b) an intercalating layer. If the intercalating layer thickness h is not resolved by the seismic pulse, the reflection is generally indistinguishable from a).*

B. Wide-angle reflection coefficient data

Seabed reflection coefficients were measured at the thick and thin mud sites (see [9] for data collection details). A trans-dimensional Bayesian inversion method was applied to data 400-1250 Hz at both sites [13]. Rather than employ a traditional geoacoustic parameterization of sound speed, density and attenuation, a causal sediment acoustics model was employed, the Viscous Grain Shearing (VGS) model [14]. In this approach, the VGS parameters are inferred directly from the reflection data, then sound speed, density and attenuation are computed from these parameters at arbitrary frequencies. The significance of this is that the frequency dependence of the sound speed and the attenuation are constrained to be physically possible, i.e., do not violate causality both inside and outside the measurement band.

Porosity is the most sensitive VGS parameter to the reflection data and is shown at the thick and thin mud sites in Figure 3. The probability density is indicated by color, with warm colors (e.g., red) indicating high probability and cool colors indicating low probability. As an indication of the high sensitivity of porosity to the reflection data, at 0.16 cm depth (thick mud site) the mean porosity is 0.64 with 95% highest probability density credibility interval (CI) of [0.63 0.66]. It is important to note that the inversion method (see [13] for details) presumes iso-porosity layers. Thus, the stairstep profile may represent a discrete layered medium or continuous gradients or a combination of both. At the thin mud site, measured porosity from a vibracore agrees closely with the inferred porosity (see Fig 12 in [13]).

The sediment sound speed profiles are also shown in Figure 3 (right-hand side) which are computed from the full posterior probability density (PPD) of the VGS parameters. The mean (solid line) and 95% CI (thin dashed lines). As an example of the small uncertainties in the sound speed, at 0.16 m depth (thick mud site), the mean is 1453 m/s with 95% CI of [1446, 1458] m/s.

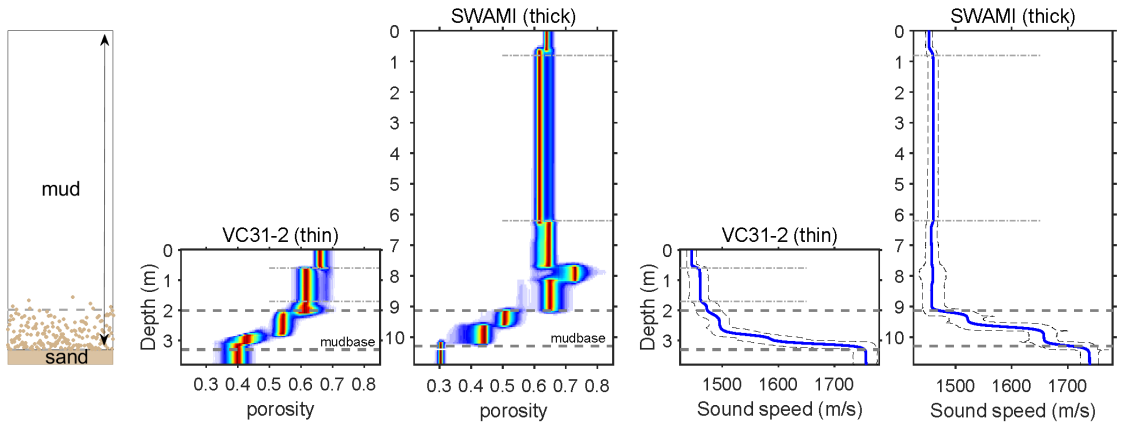

Figure 3. *Mud layer structure. From left to right: cartoon illustrating sand-mud transition interval, porosity profiles at two sites (thin and thick mud layers) and sound speed profiles (450 Hz) at the same two sites. The mud layer is defined from the water-sediment interface (0 m) to the mudbase (lower dashed line). Within the mud layer there are two intervals, a quasi-homogeneous mud interval from the water-sediment interface to the top of the sand-mud transition interval (upper horizontal dashed line) and the sand-mud transition interval characterized by a decreasing porosity and increasing sound speed to the mudbase. Below the mudbase is sand. The plots are aligned at the mudbase to highlight the similarity of transition interval at two disparate sites. Two sub-intervals are indicated by dash-dot lines: a surficial mud sub-interval within the upper meter, and a homogeneous mud sub-interval in which the properties are virtually constant. The bottom water sound speed is 1471 and 1474 m/s at the thin and thick mud site respectively. (Color online)*

The porosity and sound speed profiles suggest two distinct geoacoustic intervals within the mud layer, which is defined from the water-sediment interface to the mudbase (lower gray dashed line). The inferred mudbase horizon from the reflection data is in very close agreement (within ~0.1 m) with interpolated two-way travel time from sub-bottom profiler data [11] using the sound speed profile in [13].

Above the mudbase, the porosity rapidly increases and the sound speed rapidly decreases. When the inversion results were first examined, the authors of [13] were unaware of why the porosity and sound speed showed such strong gradients, in other words there was no prior information about the existence of such strong gradients. Work from Goff et al. [11] and Chaytor et al. [12], however, revealed that the sand from below the mudbase had become entrained in the mud above the mudbase caused by a mixing process, at first believed to be due to storm events and at present believed to be caused by biologic mixing [15] and sea-level fluctuations. This sand-entrained mud, ~1 m thick, is termed the sand-mud transition interval; a cartoon of this interval is shown in Figure 3. The adjective ‘sand-mud’, rather than ‘mud-sand’ is chosen to describe the transition interval to emphasize that sand is entrained in mud, and not the other way around. Nevertheless, for brevity, the term ‘sand-mud transition interval’ will be shortened to ‘transition interval’ in most of the remainder of the paper. The sand content in the transition interval is greater than 50% [12] and drops to less than 20% [12] above the transition interval ,which has a profound effect on the sound speed which decreases ~200 m/s in ~1 m. The top of the transition interval is determined in this study principally by the sound speed profile, i.e., where sound

speed becomes nearly constant. At the thick mud site, the top of the transition interval corresponds to the mh1 seismic horizon, the first seismic horizon above the mudbase. The mh1 horizon does not appear at the thin mud site.

From the top of the transition interval (upper gray dashed line) to the water-sediment interface is termed the quasi-homogeneous mud (qHm) interval. In this interval, the porosity and sound speed variability is rather modest. At the thick site, the largest variation is in the porosity between 6.2 and 9 m, yet the sound speed is nearly constant varying by less than 5 m/s from 1460 m/s. The variability at 8.2 m and 6.2 m correspond closely to Goff's mh2 and mh3 horizons respectively. Seismic mud horizons mh4 and mh5 do not correspond to any features in the inferred porosity or sound speed profiles, with the exception that at the thin mud site there is weak evidence in the porosity of a horizon about 0.2 m above the top of the transition interval which closely corresponds with mh5. A reasonable explanation is that mh4 and mh5 are thin intercalating layers of the type in Figure 2b which are not resolved in the lower bandwidth reflection coefficient data. Chaytor et al. [12] also note that there is no feature in the core data corresponding to mh5.

Two sub-intervals in the quasi-homogeneous mud interval are also identified (indicated by the gray dash-dotted lines, Figure 3): the upper ~1 m, which has a higher porosity and lower sound speed, is defined as the surficial mud sub-interval, and a sub-interval below this in which the porosity is constant which is termed the homogeneous mud sub-interval.

C. Core data

Extensive coring was undertaken in the NEMP area, including piston cores, gravity cores, vibracores and acoustic cores [16]. Chaytor et al. [12] provide analysis from an extensive subset of those cores, identifying three geologic units. The uppermost geologic unit, Unit 1, is predominantly a sand-clay-silt with mean constituents (by weight) of respectively 19%-25%-56%. The consistent lithology in Unit 1 results in a very tight range of porosity and grain density values, with a mean porosity of 0.60 and standard deviation of 0.04 [12]. A sub-unit, Unit 1a, is also identified, extending from the water-sediment interface to as deep as ~2 m with a slightly larger grain size (higher silt concentration), though this unit it does not appear in every core and is treated as tentative. Unit 1a may be related to the surficial mud sub-interval defined above, though a larger grain size generally would imply a lower porosity, which is not what is observed. The lower depth bound of Unit 1 is determined by an increasing sand content. Thus, the geologic-based Unit 1 ostensibly corresponds to the combined (geoacoustic-based) surficial mud and homogeneous mud sub-intervals. One notable feature of Unit 1 is the near absence of grain sizes greater than 63 μm; randomly distributed shell fragments constitute the entire gravel fraction at a mere 0.03% by weight [12].

The principal characteristics of Unit 2 are an increase in silt and sand and a decrease in the smallest component of clay constituents; hence, relative to Unit 1, an increase in mean grain size. The sand fraction increases with depth in Unit 2 as do shell fragments with numerous shells at its base in some cores, with some individual shells larger than 4 mm. In addition, heterogeneity increases with silt and clay fractions varying substantially with depth [12]. Unit 2 ostensibly corresponds to depths between the homogeneous mud sub-interval base and the mudbase. Unit 3 is the transgressive sand sheet.

The geologic divisions from the cores are clearly different than the geoacoustic-based divisions primarily used in this paper. This can be understood because there is a complex relationship between the geologic parameters (e.g., grain size, mineralogy) and sound speed, for example. Thus, it is not surprising that geologic units and geoacoustic intervals are related, but not the same.

III. MUD LAYER ATTENUATION

In-situ attenuation results in mud are presented from several kinds of data, including seabed reflection, long-range propagation and reverberation and using several inversion techniques. Results are compared within the New England Patch and with observations at other shallow water locations.

A. Bragg interference decay (NEMP, thick mud)

A new approach is developed and used here to estimate attenuation, based on exploiting the frequency dependence of low grazing angle seabed reflection-coefficient data, as shown in Figure 4. One of the salient characteristics of the data are the interference fringes that are bunched more tightly near normal incidence (90°). These fringes or oscillations are due to the constructive and destructive interference between waves reflected from the top and bottom of a layer and are governed by the Bragg's law where for a sediment layer j, $k_j d_j \sin(\theta_j) = n\pi$, where k is the wavenumber, d is layer thickness, θ is grazing angle, and n is an integer. For purposes here, it is noted that the frequency-dependent decay of the Bragg interference pattern for a layer is quite sensitive to the attenuation in that layer. Thus, the attenuation information is primarily in the frequency-dependent slope of the Bragg interference oscillations.

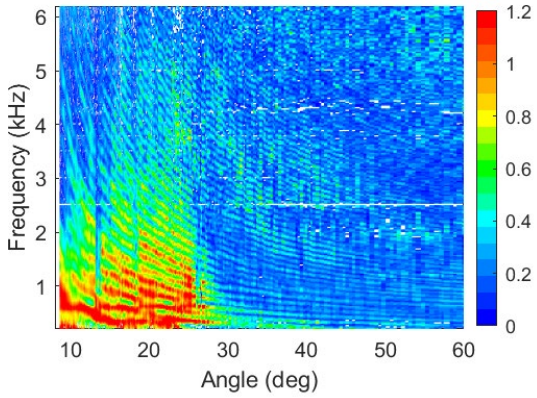

Figure 4. *seabed reflection coefficient measurement at the thick mud site with a 25 Hz averaging bandwidth. (Color online)*

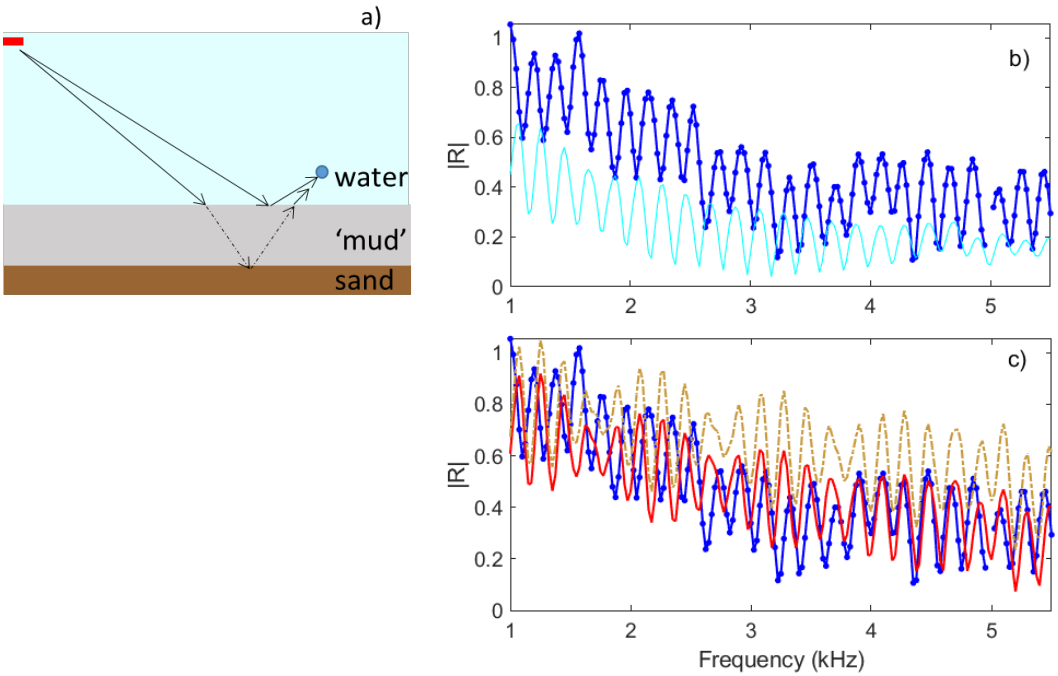

Figure 5. *a) cartoon (not to scale) of reflected paths from the top and bottom of the ~10 m thick mud layer that leads to phase interference. Measured (solid line with dots) and modeled reflection coefficients at 21.5° at the thick mud site, b) mud layer attenuation 0.1 dB/m/kHz (solid line), c) mud layer attenuation 0.02 dB/m/kHz (dash-dot) and 0.04 dB/m/kHz (solid line). (Color online)*

For the highest sensitivity to the mud attenuation, it is useful to choose an angle that is below the (sand) critical angle, firstly because low angles have a longer path through the mud layer, hence higher losses due to the attenuation, and secondly because the structure below the mud (where the acoustic field decays exponentially) is less important to the mud attenuation inference.

The oscillations as a function of frequency at a given angle are clearly seen in the reflection data (Figure 5b, line with filled circle marker at each data point). The scalloped shape of the oscillations (broad peaks and narrow nulls) arises from the absolute value operator on the reflection coefficient. The oscillations are primarily due to the interference between the water-mud interface and mud-sand interface reflected paths, see ray diagram in Figure 5a. The data, Figure 5b, exhibit two main components: rapid variations with a period of ~200 Hz, and slowly decaying amplitudes.

The decaying amplitudes can be explained as follows. The amplitude of the water-mud interface reflection is ~0.23 independent or nearly independent of frequency. Since the reflected path from the mud-sand interface transits twice through the 10 m mud layer (Figure 5a) it loses energy due to attenuation in the mud layer, i.e., its amplitude decreases with increasing frequency. The energy impinging on the mud-sand interface is below the critical angle, and thus at sufficiently low frequencies (e.g., 1 kHz) the reflection coefficient is ~1. In fact, over much of the frequency range, the mud-sand reflected amplitude is larger than that from the water-sediment interface. Thus, the water-mud reflected path phase interference is visible as a modulation on the gradual decrease in the reflection amplitude.

It is clear from the forgoing discussion that the reflection data are sensitive specifically to the average attenuation in the mud layer; that attenuation is estimated here via forward modeling. While ray theory was used above to give some insight into the Bragg interference, the reflection coefficient model employed here includes full-wave physics including all multiples within a layer, wave diffraction and non-planar wavefronts which give rise to Fresnel zones. In essence, the reflection coefficient model is the Sommerfeld-Weyl integral (e.g., [17]) normalized by the incident specular field (e.g., see Eq. 4, [9]). The reflection coefficient model is sufficiently complex in order to account for all the relevant physics. The attenuation is inferred from the modeled reflection coefficient via visual evaluation of the data fit over a fairly wide scale (i.e., a reasonably good attenuation value and values that are clearly too high and too low were straightforward to establish). More sophisticated inverse methods could be applied, but the simple approach is sufficient to both demonstrate the method and to provide a sanity check on the more complex Bayesian inversion result. An initial attenuation value of 0.1 dB/m/kHz predicts a decay rate far larger than that of the data (cyan line, Figure 5b). Instead, a mud attenuation of 0.04 dB/m/kHz yields a reflection coefficient decay rate comparable to that of the data (Figure 5c, red line). To give an indication of data sensitivity, an attenuation of 0.02 dB/m/kHz is also shown (Figure 5c, dash-dot brown line), which clearly shows a decay rate that is too low.

To improve sensitivity and better estimate uncertainties, the measured data and model results are averaged over a larger bandwidth, 350 Hz from 0.5-6.5 kHz, see Figure 6. The uncertainties are given here as approximate outer attenuation bounds {0.03 0.055} dB/m/kHz where below and above these bounds, the observed decay rates are poorly predicted. With these bounds, the results at this site, 0.04 {0.03 0.055} dB/m/kHz, can be compared with Bowles [4] empirical relationship at 3.5 kHz (the center of this analysis band) that yields 0.064 dB/m/kHz, which is considerably smaller than the Hamilton estimate of 0.4 dB/m/kHz. Nevertheless, it is clear that the Bowles estimate is also too high for the NEMP mud, i.e., higher than the upper bound, 0.055 dB/m/kHz, which itself is too high (Figure 6).

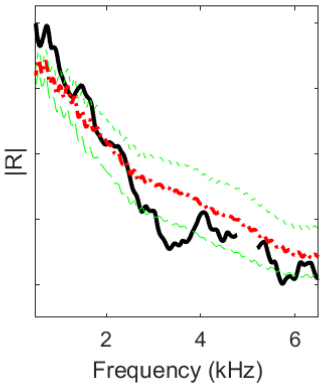

Figure 6. *Measured (heavy solid line) and modeled reflection coefficients at 21.5° smoothed over a 350 Hz bandwidth at the thick mud site. Modeled mud attenuation at 0.04 dB/m/kHz (dash dot), 0.055 dB/m/kHz (long dash), 0.03 dB/m/kHz (short dash). (Color online)*

In estimating the attenuation using the Bragg spectral decay, the sediment sound speed profile from the Bayesian inversion was employed. However, assuming an iso-velocity mud layer (i.e.,

ignoring the sound speed gradient in the transition interval) yields the same attenuation estimate. This is because the turning point in the transition interval is quite close to the mud boundary and thus the path lengths (with or without the sound speed gradient in the transition interval) are very nearly the same.

In the forward modeling described above it is necessary to assume a form of the attenuation frequency dependence. This is so because the relatively sparse data employed are not sufficiently informative to justify using a more sophisticated approach. Based on Hamilton [2] and Bowles [4], a linear frequency dependence is assumed. It can be noted that the assumption seems reasonable, inasmuch as the linear frequency dependence fits the data reasonably well over a range of more than three octaves (Figure 6). In summary, the attenuation estimated from the reflection data is 0.04 {0.03 0.055} dB/m/kHz from 0.5-6.5 kHz.

B. Bayesian reflection coefficient inversion (NEMP, thick mud)

The above attenuation estimate, 0.04 dB/m/kHz, derived from simple physics and forward modeling (first reported in 2017 [18]) can be used as a sanity check on the attenuation inferred from the more complex trans-dimensional Bayesian inversion method [13] at the same site. That study used reflection coefficient data at steeper angles (25°– 60°), i.e., there is no overlap in the angular range, and a frequency range 400-1250 Hz. As previously noted, rather than employ a traditional parameterization of sound speed, density and attenuation, a causal sediment acoustics model (VGS) was employed [14] so that the VGS parameters (estimated over the frequency range of the measured data) can be used to extrapolate sound speed and attenuation to other frequencies without violating causality.

In Figure 7a, the attenuation predicted from the inferred VGS parameters is shown within (red) and outside (gray) the reflection coefficient measurement band. This curve was generated by converting the depth-dependent PPD of the VGS parameters to attenuation at 0.1 m increments in the mud layer (0 to 10.3 m depth). The mud layer-averaged attenuation was formed (gray line) from this ensemble. The attenuation estimated from Bragg oscillations is shown in the blue dotted line. The same information is presented more clearly in Figure 7b by dividing by frequency. In these units, it can be clearly seen that the mean Bayesian results indicate a nearly linear frequency dependence which is an important result. A second important result is that the Bayesian estimates are close to that from the Bragg interference decay. The uncertainties will be shown and discussed in Sec III.E.

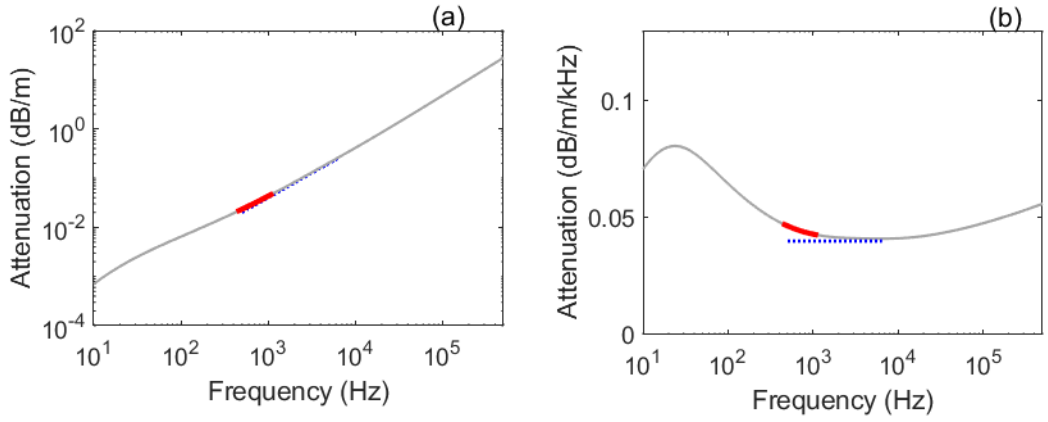

Figure 7. *a) estimated layer-averaged attenuation for the mud layer from Bragg oscillations (dotted line), and from Bayesian wide-angle reflection coefficient inversion (thick line over the measurement band, gray line extrapolated outside this band). b) Same quantities as in a) but scaled by frequency. (Color online)*

C. Layer-averaged attenuation - comparison factors

It is desirable to compare these results to other attenuation estimates at the NEMP. However, strictly speaking, layer-averaged attenuation cannot be directly compared between different sites if mud layer thickness (from the water-sediment interface to the transgressive sand boundary) is different. This is so because the transition interval has a much larger attenuation than the intervals above it; thus, the ratio of the transition interval thickness to total mud layer thickness plays a role in the layer-averaged mud-layer attenuation. In other words, the layer-averaged mud attenuation is expected to be larger at thin mud sites than in thick-mud sites.

Here we attempt to separate attenuation in the transition interval (with an average of 52% sand) from attenuation in the mud above it (average of 19% sand) using depth-dependent attenuation results from [13]. Depth-dependent sound speed and attenuation at the thick mud site estimated from reflection data in [13] are shown in Figure 8a,b. Having both the sound speed and attenuation results side-by-side is useful for discussion. The attenuation, Figure 8b, decreases in the upper meter, below which it is constant in the homogeneous mud sub-interval (1– 6.2 m) at ~0.013 dB/m/kHz, Figure 8c. At deeper depths, and unlike the sound speed (which is nearly constant), attenuation exhibits strong depth-dependence between 6.2 m and the top of the transition interval, 9.1 m. Some of that structure is likely artifacts, for example the high mud attenuation between 8-9 m, and especially the thin dip near the transition interval. As previously mentioned, attenuation estimates in thin layers are generally poor because the information content is poor. The dip is not only thin, but it occurs in a complex region of parameter space with rapidly varying sound speed and porosity. Taking this into account, attenuation in the qHm interval is ~0.025 dB/m/kHz, and considerably higher in the transition interval, ~0.17 dB/m/kHz.

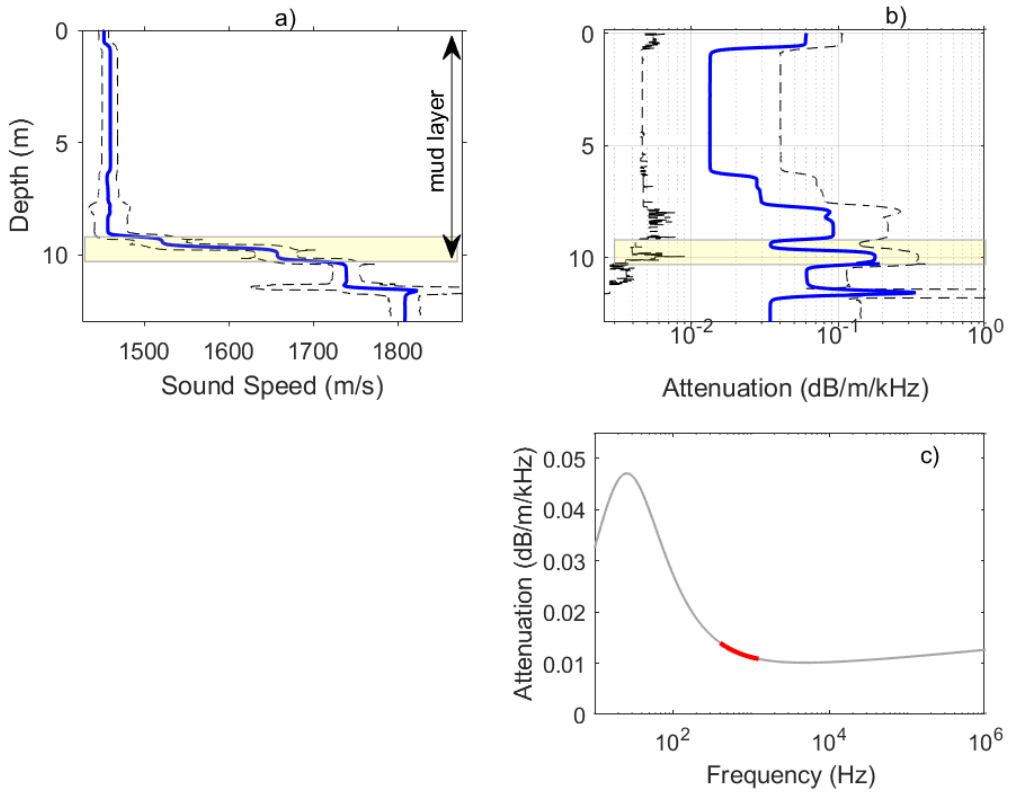

Figure 8. *Bayesian inversion for geoacoustic properties via VGS parameters at the thick mud site; solid lines in each plot represent the mean, the dashed lines are the 95% HPCI. The transition interval is shown in shaded box. a) sound speed at 450 Hz, b) attenuation at 450 Hz, c) attenuation from 1 – 6.2 m (measurement band shown in thick line). (Color online)*

The mud layer-averaged attenuation $\bar{a}$ can be expressed as

$$\bar{a} = \sum_{i=1}^{N} a_i d_i \Big/ \sum_{i=1}^{N} d_i \qquad (1)$$

where a_i and d_i are the attenuation and thickness in the i^{th} interval. The averaging depth can be sub-divided into an arbitrary number of intervals or sub-intervals N. Here N=2 suffices, the qHm interval and the transition interval. This simple depth scaling allows layer-averaged attenuation results to be compared at various mud thicknesses.

For simplicity, two assumptions are initially made: that a_1 and a_2 of the qHm and transition intervals are constant across the NEMP, and that d_2 =1.2 m is also constant. The former assumption requires that the mud fabric above the transition interval be more or less uniform across the NEMP, which may not be unreasonable given that the mud was deposited in a relatively low energy environment. The latter assumption presumes that the biologic mixing rate and the mud deposition rate were more or less constant over time. Neither of these assumptions are required but seem reasonable at the NEMP.

Given these assumptions, the spatial variation in the mud layer-averaged attenuation $\bar{a}$ can be estimated solely from the depth of the mudbase, $d_{mb}= d_1 + d_2$, which is given by the sub-bottom

profiler data. As an example of how mud layer thickness affects layer-averaged attenuation, a 4 m mud layer thickness (d_{mb}=4 m) would yield a 0.07 dB/m/kHz layer-averaged attenuation, i.e., nearly double the layer-averaged attenuation of the 10 m thickness.

D. Bragg and Bayesian inversion (NEMP, thin mud)

The hypothesized mud layer spatial dependence can be tested by comparing attenuation from the thick mud (SWAMI) with that at the thin mud site, (VC31-2, see Figure 1) where the mud layer thickness is only 3.2 m. Physics dictate that inferring attenuation is more challenging at the thin mud site because the path length in the mud is shorter by a factor of 3. That is, generally the thinner the layer, the larger the attenuation uncertainties.

Assuming the same a_1, a_2 and d_2 as at the thick mud site and $d_1 = d_{mb} - d_2 = 2$ m, the mud layer-averaged attenuation at the thin mud site is predicted to be $\bar{a}$ =0.079 dB/m/kHz. This is first compared with the estimated attenuation from the Bragg oscillation decay. From the reflection coefficient data, Figure 9a, an angle is chosen below the apparent critical angle (33°); forward modeling shows that a layer-averaged attenuation of 0.08 dB/m/kHz yields good agreement with the Bragg spectral slope decay, Figure 9b. The similarity of this result with the depth-scaled prediction is consistent with a_1, a_2 being similar between the two locations.

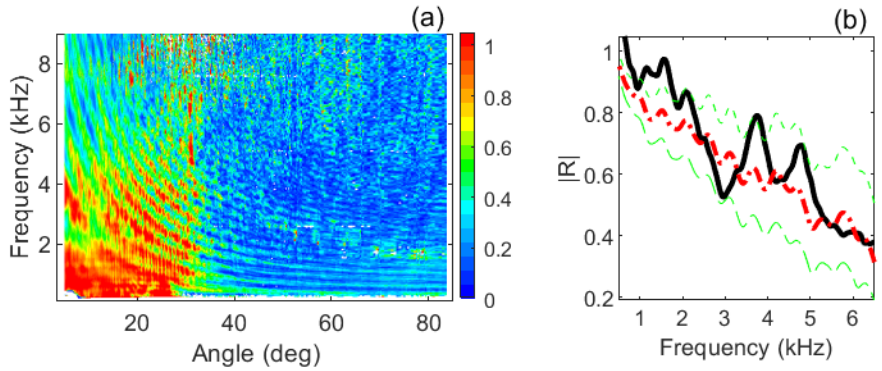

Figure 9. *a) measured reflection coefficient data at the thin site, b) measured (thick solid line) and modeled reflection coefficients at 26° smoothed over a 600 Hz bandwidth. Modeled mud attenuation at 0.08 dB/m/kHz (dash-dot), with outer bounds of 0.04 dB/m/kHz (short dashed), 0.13 dB/m/kHz (long dashed). (Color online)*

In order to examine the mud attenuation structure more closely, the depth-dependent Bayesian inversion results are employed, Figure 10. It should be first noted that the large spike in attenuation at the top of the transition interval (2 m), Figure 10b, seems unreasonable (a thin and unreasonable feature was also observed at the thick mud site at the top of the transition interval). The spike is not only thin, but it occurs in a complex region of parameter space with rapidly varying sound speed and porosity. Furthermore, in the transition interval below the spike, attenuation is unreasonably low given the high sand content. What appears to be happening is that the high attenuation at the upper and lower boundaries of the transition interval and the low attenuation within the transition interval are self compensating to give an average value of ~0.16 dB/m/kHz within the transition interval, similar to that at the thick mud site.

Secondly, the attenuation in the qHm interval is comparable to that at the thick mud site, ~0.025 dB/m/kHz (0 – 1.75 m). Finally (which must be true given the above) the layer-averaged

attenuation over the mud layer (0–3.2 m) is 0.076 dB/m/kHz, nearly the same as that predicted from the thick mud site, and that estimated from the Bragg interference decay, $\bar{a}$ ~0.08 dB/m/kHz. These similarities indicate that the interval attenuations are reasonably similar from these two sites separated by ~15 km, with mud thickness differing by a factor of 3, and where the formation of the transition interval occurred at different geologic times (when the transgressive sand sheet was formed, VC-31-2 was at a higher elevation than SWAMI and due to mud deposition dynamics, lowest regions are filled first; hence the mud was deposited VC31-2 later than that at SWAMI).

The fact that the interval attenuations a_1 and a_2 are each consistent between the thick and thin mud sites, suggests that the detailed properties of the mud that control attenuation are also reasonably similar. It also may suggest that the attenuations are similar across the New England Mud Patch. Some differences between sites may exist, for example the homogenous mud sub-interval attenuation is somewhat higher at the thin site, 0.02 dB/m/kHz, than the thick site, 0.013 dB/m/kHz, but the uncertainties are such that the two values may not be statistically distinguishable.

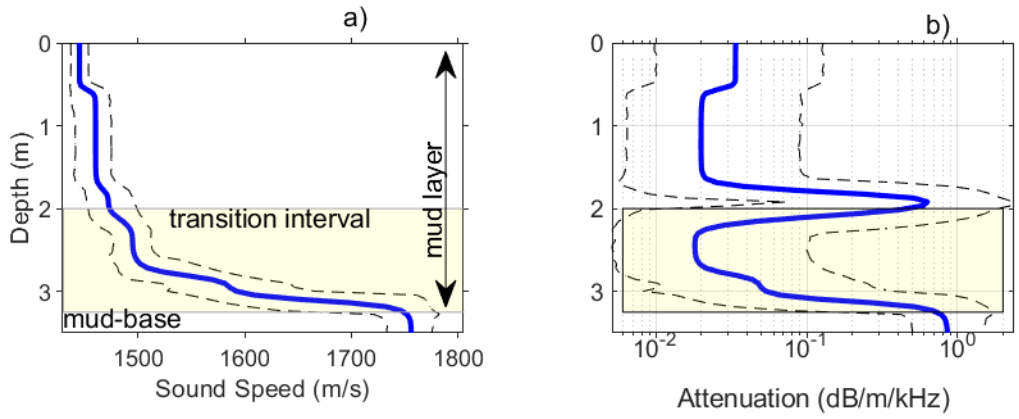

Figure 10. *Bayesian inversion of geoacoustic properties via VGS parameters at the thin mud site from [13], a) sound speed at 450 Hz, b) attenuation at 450 Hz, Solid lines in each plot represent the mean, the dashed lines are the 95% HPCI. The transition interval is shown in the shaded box, and the mud layer defined from the top of the sediment to the mud-base. (Color online)*

E. Modal inversion (NEMP, thick mud)

Mud attenuation in the NEMP was estimated at 150 Hz by calculating the modal attenuation coefficient from the first mode out to ranges from ~7-15 km [19]. The receive array used in this study was ~1 km WNW of that used at the thick mud site (Sec. III.B), and the bearing of the tracks in [19] were roughly WNW to NW. The mud layer thickness varied over the two propagation paths, with an average of 9.55 m. For comparison with the thick mud site in Sec. III.A (mud layer thickness of 10.3 m), the depth scaling, Eq.(1) is used to estimate the effect of different mud layer thickness between the two data sets: $\bar{a}(9.55m) - \bar{a}(10.3m) = 0.0008$ dB/m/kHz. This is so small relative to the uncertainties that no depth scaling needs to be performed to account for the difference in mud layer thickness between the two data sets; i.e., the modal estimate can be directly compared with the thick mud measurement.

The first mode was chosen inasmuch as it was most sensitive to the mud layer and least sensitive to sand layers below it [19]. The resulting mud layer-averaged attenuation is 0.006±0.003 dB/m at 150 Hz, or $\bar{a}$=0.04±0.02 dB/m/kHz at 150 Hz, Figure 11 (x). A few comments should be made about the uncertainties from the various measurements. The uncertainties are critical for making reasonable comparisons and conclusions, but, as often the case, the uncertainties represent somewhat different things. In the modal inversion results, the uncertainty is the standard deviation from five source pulses (explosives) at multiple ranges and bearings averaged over lateral spatial scales of order 10 km. The Bayesian reflection coefficient inversion results (gray and red) represent the mean and standard deviation from the mud layer-averaged attenuation over lateral scales ~70 m. The attenuation uncertainties from Bragg interference decay (blue) is not a standard deviation, but rather limiting bounds based on forward modeling (see Figure 6), and are considered as an upper bound to the standard deviation.

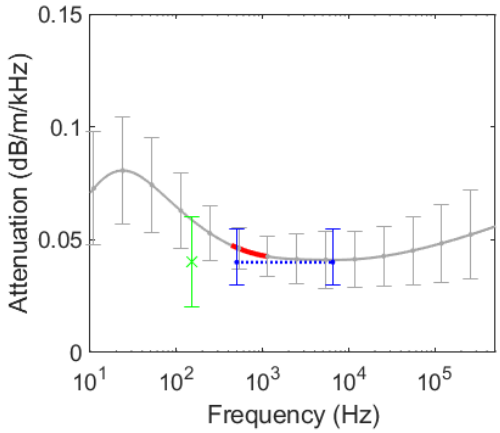

Figure 11. *mud layer-averaged attenuation at/near the thick mud site: forward modeling of Bragg oscillations (dotted line); Bayesian inversion for VGS parameters (solid); same but limited to the measurement band of the reflection coefficient (thick solid); inferred from first mode of long-range propagation data (x). (Color online)*

Measurements at three locations, SWAMI, VC31-2, and this long-range propagation measurement support the conjecture that the interval attenuations a_1 and a_2 are similar across the NEMP.

F. Bayesian reflection coefficient inversion (Malta Plateau)

Prior to this present work, the existence and role of the sand-mud transition interval on attenuation had not been understood. In the present study, the authors have come to realize that a transition interval exists at the base not only at NEMP, but likely in virtually all shallow-water mud deposits. Thus, it is of interest to review earlier work in a different shallow-water water muddy continental shelf, the Malta Plateau, with intent to examine the transition interval effects there.

Layer-averaged attenuation through a 10 m mud layer was estimated to be 0.009 [0.006 0.013] dB/m/kHz (mean and 95% CI) at 1 – 3.6 kHz [6]. The data were collected at the Malta Plateau in 100 m water depth near a location termed Site 4. This attenuation value is considerably smaller than that at the NEMP (SWAMI), 0.04 dB/m/kHz {0.03 0.055} over the same mud thickness.

In order to address the attenuation difference, the characteristics of the sand-mud transition interval at Site 4 were sought. Though details of the Site 4 transition interval are not available, nearby sites (Site 2 [20], and Site 16 [21] separated by 14 km) show a clear transition interval at the base of the mud. The thickness of the transition interval is ~0.35 m at both sites. These are valuable observations because first they show that the transition interval exists in a different geologic setting, and second they support the conjecture that the transition interval thickness is roughly constant in a given region. The Malta Plateau transition interval thickness is a factor of 3 smaller than that at NEMP due to faster deposition and/or slower biologic mixing rates. This means that the impact of the transition interval on layer-averaged attenuation will be smaller at the Malta Plateau. Furthermore, the Malta Plateau transition interval attenuation, a_2, at the two sites appears to be roughly half that at NEMP, see Fig. 9 in [20] and Fig. 9 in [21]. This lower value can be explained by the fact that higher deposition rates and/or lower mixing rates means lower sand content, which leads to a lower attenuation. If the Site 4 transition interval thickness and attenuation were similar to the other two nearby sites, d_2=0.35 m a_2=0.075 dB/m/kHz, then the mud attenuation above the transition interval would be ~0.0066 dB/m/kHz, reasonably close to layer-averaged value $\bar{a}$=0.009 dB/m/kHz. The salient point is that the transition interval has less effect on layer-averaged attenuation in regions with high mud deposition rates and/or low biologic mixing rates because the transition interval will be both thinner and lower in attenuation.

IV. DISCUSSION

The layer-averaged attenuation is a valuable observation in its own right and when combined with depth-dependent attenuation has helped shed light on the role of the transition interval. In this section, the transition interval, the attenuation depth dependence and frequency dependence are discussed.

A. Role of the sand-mud transition interval

It is clear that the sand-mud transition interval plays a significant role in mud layer attenuation at the New England Mud Patch. Since the transition interval exists because of biologic (mixing) and geologic (deposition) processes that are virtually ubiquitous [15], it is concluded that the transition interval may also exist in all, or at least many, muddy continental shelves. The characteristics of the transition interval, however, may vary widely depending upon the processes local to that region.

From the standpoint of predicting acoustic propagation on the continental shelf, the layer-averaged mud attenuation is an important parameter. This is true because the mud layer (including the transition interval) is part of the waveguide. Therefore, the layer-averaged mud layer attenuation is a significant contributor to the frequency dependence of the propagation. Thusly, it can be concluded that the existence of the sand-mud transition interval likely plays an important role in acoustic propagation in many muddy continental shelves.

Our data, though limited, indicate that the attenuation within the transition interval is reasonably consistent across large distances on a given shelf, as is the attenuation in the mud above the transition interval. Thus, if the mud layer and transition interval thicknesses are known, it may be possible to predict the variable layer-averaged attenuation across the region – reflecting the significant changes in layer-averaged attenuation associated with changes in mud layer thickness.

It is sometimes desirable to make predictions of sound propagation in regions in which no acoustic/geoacoustic data are available. In muddy continental shelf areas, the understanding developed here forms the basis for predicting the attenuation. The purpose of this section is to convey the high-level idea, the details have not been worked out.

In its simplest form, the layer-averaged attenuation in a muddy layer is $\bar{a}=(a_1 d_1+a_2 d_2)/(d_1+d_2)$, where subscripts 1 and 2 indicate the mud above the transition interval and the transition interval respectively. The transition interval thickness d_2, in principle, can be estimated taking into account sea-level variations and the ratio of mixing to deposition rates. The transition interval attenuation a_2 can also be estimated empirically from this same ratio since when the ratio is small, the transition interval is thin with a relatively low percentage of sand and therefore lower attenuation, e.g., as observed in the Malta Plateau. With additional data, improved empirical relations and/or theoretical predictions can be developed. In the mud above the transition interval, a_1 can be estimated from best-available empirical relations and d_1 from mud thickness isopach maps not infrequently available based on sub-bottom profiling surveys.

As an example, a prediction of mud layer-averaged attenuation at the NEMP is shown in Figure 12a. This is expected to be more accurate than what is currently assumed, using either Hamilton [2],[3] or Bowles [4] empirical relations. By explicitly accounting for the transition interval, the layer-averaged attenuation exhibits an increase towards the edges of the experiment area, where the mud layer thins, see Figure 12b. This has been observed at the NEMP, see Sec III.D. Other muddy continental shelves regions around the world will exhibit different mud accommodation spaces (three-dimensional shape of the mud unit), but the layer-averaged attenuation spatial variability should follow the same trends, e.g., the lowest attenuation would be observed in the thickest regions of the mud.

It is of interest to compare Figure 12a with what could have been predicted with no prior knowledge. A primary tool used for such predictions is the empirical relations of Hamilton [2],[3] or Bowles [4]. It should be noted firstly that the predicted attenuation value from either one is constant across the NEMP, whereas in reality the attenuation varies by a factor of 3, 0.04 −0.012 dB/m/kHz. Bowles' relations (which can be considered the state-of-art) require selection of one his two values 0.004 or 0.026 or perhaps the mean, 0.015 dB/m/kHz. In the absence of any prior knowledge, the mean would be a reasonable choice. Yet the mean, 0.015 dB/m/kHz (and either bound) is far below the NEMP values, 0.04 −0.012 dB/m/kHz. Hamilton predicts a spatially constant value of 0.4 dB/m/kHz, which is far above the NEMP values. The point is that the sand-mud transition interval has a substantial affect in terms of the attenuation magnitude and its spatial variability, neither of which are included in the current empirical models.

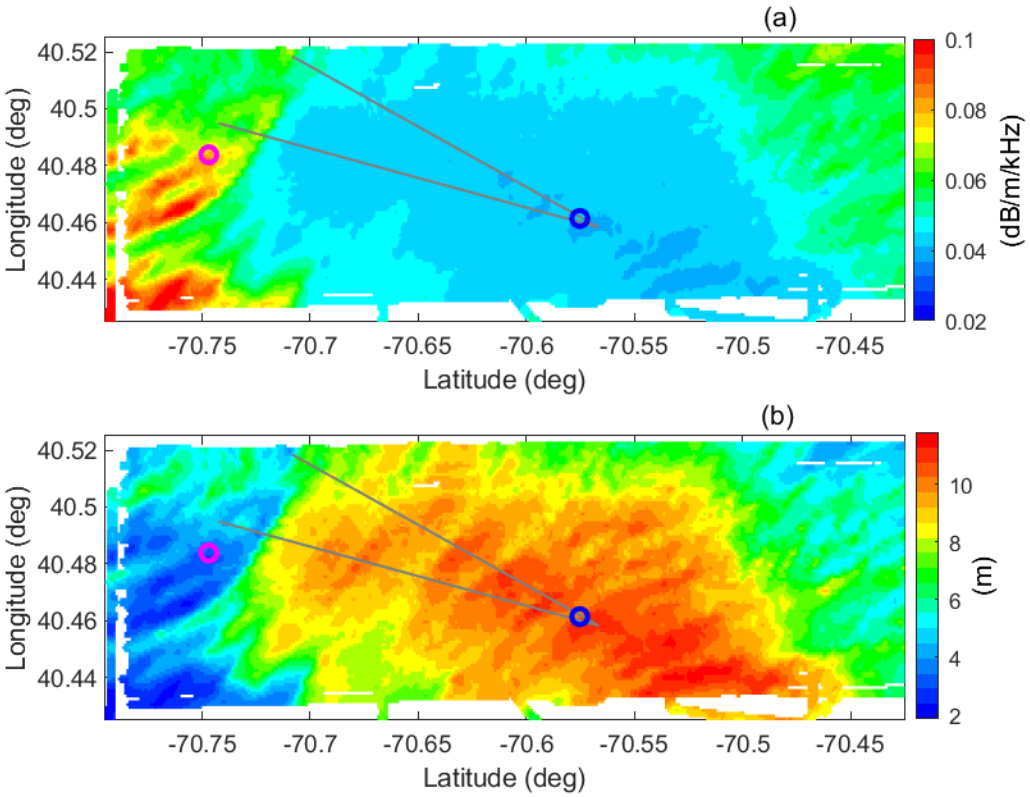

Figure 12. *NEMP mud layer: a) layer-averaged attenuation and b) thickness [11]. The locations of the reflection-derived attenuation estimates are shown at the thin mud (western circle) and thick mud (central circle) sites and the mode-derived estimates (gray lines). (Color online)*

Depending on the acoustic models applied, the attenuation parameterization can be more realistic by explicitly treating one aspect of the depth dependence. That is, instead of a mud layer-averaged metric, the mud-layer is treated as a two-interval unit where the two intervals are the sand-mud transition interval and the quasi-homogeneous mud interval. As an example, Figure 13 shows a slice through the three-dimensional volume at the NEMP.

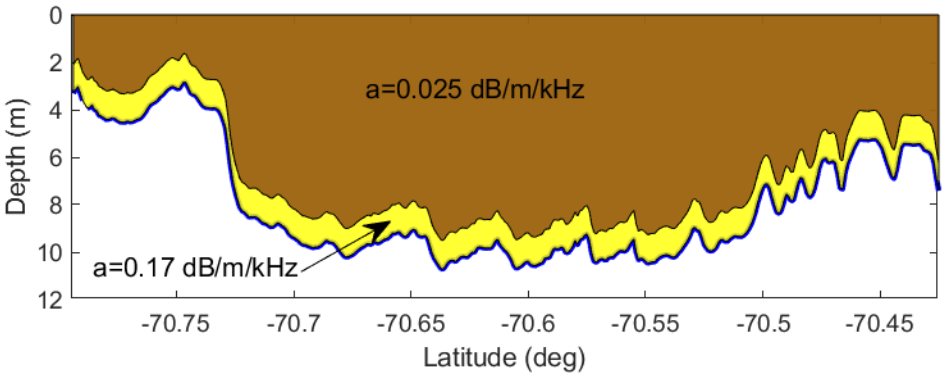

Figure 13. *A two-interval mud layer model of attenuation at the NEMP (cross section at latitude 40.48° N). (Color online)*

Inner shelf mud deposits may require a different approach when the mixing-to-deposition rate ratio is high and where episodic flooding events include large quantities of sand, e.g., the Amazon River delta, see [15]. In this case, instead of a homogenized sand-mud transition interval, the sediment column will be composed of distinct interbedded layers of sand and mud. In this sedimentary environment, the notion of layer-averaged attenuation is not valid since the layers impose a complex frequency dependence on acoustic propagation through the layered medium (one way to treat this case is via a stochastic layered model, e.g., [22]).

B. Surficial mud depth-dependence

It is interesting to note that at the thick mud site, the attenuation markedly decreases in the upper meter (Figure 8b). There is a similar behavior at the thin mud site (Figure 10b). This decrease in attenuation in the upper meter is similar to that observed in six sites on the Eel River delta sediments [7] and at both sites on the Malta Plateau (Site 2 [20], and Site 16 [21]). In all cases, the higher attenuation is correlated with a higher porosity (other factors may also be important). The observed near-surface depth-dependence may lead to clues about the attenuation mechanism(s).

C. Attenuation frequency dependence and models

The layer-averaged attenuation is a valuable observation and has helped to shed light on the role of the transition interval. However, it is not a useful observation for informing sediment acoustic models in mud because the observation includes effects of propagation through multiple distinct sediment types. That is to say, it is generally appropriate to estimate sediment acoustic model parameters for a specific homogeneous sediment layer or interval. Our interest in this section therefore is to discuss the homogeneous layer sub-interval. This interval forms a significant volume of mud at NEMP, and its relative homogeneity is suited for comparison with sediment acoustic models.

Depth-dependent attenuation results [13] have isolated VGS model parameters in the homogeneous mud sub-interval. While the VGS model was developed with granular sediments in mind, it uses high-level (time-independent and time-dependent) viscous loss functions which may be applied to any sediment. The time-independent functions lead to attenuation that go as f^2 at low frequencies up to a transition frequency, f_o, then $f^{1/2}$. At higher frequencies, time-dependent losses dominate which exhibit an $\sim f^1$ dependence. The transition frequency is entirely determined by the VGS parameter viscoelastic time constant, $\tau = 1/2\pi f_o$. This is an empirical parameter, i.e., cannot be directly measured, that can be inferred from reflection data, e.g., [20], [13]. In the homogeneous mud sub-interval, the reflection data indicate an attenuation in the 400-1250 Hz measurement band that goes nearly as f^1, see Figure 8c. Thus, the transition frequency must be at least several octaves below this band, and is estimated by the Bayesian inversion at τ =7 ms or f_o~23 Hz. The transition frequency in Figure 8c can be clearly seen at 23 Hz, with the attenuation going as f^2 below and $f^{1/2}$ above it to an $\sim f^1$ dependence.

To the authors' knowledge only one other viscoelastic time constant estimate in mud has been made [20]. This was on the outer shelf of the Straits of Sicily using reflection data from 300 – 3150 Hz. The mud thickness at that location is ~1.5 m and in the upper 1 m of mud, the average viscoelastic time constant value is τ =6 ms or f_o~27 Hz; very nearly the same as that at NEMP. This may be somewhat surprising inasmuch as the two muds are quite different. It can be pointed

out that the Straits of Sicily PPD did not indicate a clearly resolved peak, but rather a broad distribution showing that the transition frequency must be below 200 Hz (within the 95% CI).

Besides these two muds, the main value of τ cited in the literature [14], τ=0.12 ms, was derived from measurements on a clean (i.e., few clay particles) sand which is ~60 times smaller than for mud. In other words, for clean sandy sediments, the transition frequency is ~60 times higher than for this mud. The main conclusion here is that there is accumulating evidence that the transition frequency in mud is much smaller than that in sand. Having said that, it should be noted that the authors consider the values of τ ~7 ms as an upper bound, since the transition frequency ~25 Hz, was far below the measurement band, i.e., not directly observed. In order to have a more precise value of the mud visco-elastic time constant, the measured data should ideally include frequencies above and below the transition frequency. It is quite possible that the correct transition frequency is far below 25 Hz.

Finally, a suggestion is made for scaling attenuation plots to improve clarity. It is instructive to consider Figure 7. In Figure 7a attenuation varies by about 6 orders of magnitude and this is the most common way of presenting attenuation, e.g., Biot [25], Hamilton [3], Bowles [4], Buckingham [14] and many others. Tradition notwithstanding, the plot renders the information poorly. A much clearer understanding is had by scaling attenuation by one power of frequency, as is shown in Figure 7b (and Figure 8c) where attenuation varies less than 1 order of magnitude. In this format it can easily be seen that the VGS extrapolated result (gray) shows a transition frequency of ~25 Hz, where below the transition frequency attenuation goes as f^2 and above as $f^{1/2}$; then above ~150 Hz, nearly as f^1. This behavior is not at all obvious in the traditional units of dB/m, as in Figure 7a. For this reason, the authors suggest that when attenuation data and/or models are presented, they should be presented scaled by one factor of frequency. An objection might be made that the units must be dB/m so that no assumptions are made about the frequency dependence. However, this is a fallacious argument, inasmuch as plotting a quantity by a scale factor does not impose an assumption, but rather is a common and widely used tool in physics to better reveal trends in data and models. In summary, we assert that our (community) understanding of attenuation will be improved and progress enhanced by presenting attenuation with one factor frequency removed.

V. SUMMARY

The main results, discoveries and conjectures are given in the numbered list. Additional findings are also provided.

1. It was discovered that sound speed and attenuation in the lower meter of the mud layer at the NEMP is far higher than in the mud column above it. This depth interval has elevated levels of sand caused by mixing of sand (from the layer below the mud) into the mud matrix and is termed the sand-mud transition interval.

2. Measurements at two NEMP sites, one thick mud and the other thin mud, showed that the sand-mud transition interval was the same thickness at each site, that the transition interval attenuation was similar, and that the mud attenuation above the sand-mud transition interval (termed the quasi-homogeneous mud interval) was also similar. The similarity of the two disparate sites, separated by ~15 km, gave rise to the conjecture that the attenuation

in the two depth intervals were reasonably constant across the NEMP. If this is correct, the useful metric of mud layer-averaged attenuation is predictable across the entire NEMP by simple scaling with one additional piece of information, the mud layer thickness available from sub-bottom profiling data [11]. A third independent attenuation estimate at the NEMP is shown using modal analysis [19], which supports the conjecture.

3. The most far-reaching idea to come out of this work is that combined biologic and geologic processes significantly influence attenuation not only at NEMP but in perhaps virtually all muddy continental shelf areas, through creation of the sand-mud transition interval. Indeed, the role of benthic fauna, as one factor in controlling the sand-mud transition interval characteristics, may be among the most significant effects of biology on sediment acoustics below ~10 kHz. This appears to be the case at the New England Mud Patch.

4. The realization that the transition sand-mud interval may be nearly ubiquitous around the world, and the observation of the sand-mud transition interval spatial consistency across the NEMP (and likely the Malta Plateau) opens a door to predict attenuation in muddy continental shelves around the globe with a potentially modest amount of biologic (mixing rates), geologic (deposition rates and sea-level variations) and geophysical (mud-layer depth from sub-bottom profiling) information.

We have developed a new method for measuring layer-averaged attenuation using the mud layer Bragg interference decay.

- The resulting layer-averaged attenuation at a thick mud site (10.3 m) was 0.04 {0.03 0.055} dB/m/kHz from 0.5-6.5 kHz; the braces indicate outer bounds. An attenuation that varies linearly with frequency fit the observations closely. This result accorded closely with Bayesian inversion of reflection data [13] at the same site 0.045±0.009 dB/m/kHz averaged over 0.4-1.25 kHz. A mode-based inversion result [22] spatially averaging mud layer attenuation over a much larger area, ~10 km, yielded 0.04±0.02 dB/m/kHz at 150 Hz.
- The layer-averaged attenuation at a thin mud site (3.2 m) was 0.075 dB/m/kHz with outer bounds of {0.04 0.13}dB/m/kHz from 0.5-6.5 kHz.

The results indicate that mud attenuation (above the sand-mud transition interval) follows a linear or nearly linear frequency dependence from 0.15 – 6.5 kHz. The Viscous Grain Shearing parameter that controls the attenuation frequency dependence is called the viscoelastic time constant, τ. Our estimate for muds at NEMP and the Malta Plateau is $\tau \sim 7$ ms which is a factor of 60 greater than that reported for sand. This means that the attenuation in muds goes as f^2 only below a few tens of hertz or lower.

Some progress was made in addressing the question of the similarity/difference between shallow- and deep-water mud attenuation

- It is shown that in several instances, shallow-water mud attenuation can be nearly as small as that in deep-water.
- A notable difference between shallow- and deep-water is the presence of the sand-mud transition interval in shallow water, which can substantially increase the mud layer-averaged attenuation.

Results pertaining to sediment acoustic models:

- Mud layer-averaged attenuation values should be used with considerable caution in theoretical models of sound propagation through mud. Caution is required because the attenuation may be heavily influenced by the transition interval in ways that are difficult to precisely account for.
- Attenuation in homogeneous mud ranged from 0.01– 0.02 dB/m/kHz at two sites separated by ~15 km. These attenuation values may be useful for development of sediment acoustic models (e.g., [24]), particularly at the thicker mud site.

Though current empirical models predict that muddy sediment attenuation increases with increasing depth, our results at NEMP (both sites) show that attenuation decreases with depth in the upper meter. We note that the same behavior has been observed in 6 sites on the Eel River delta, and all (2) sites on the Malta Plateau. Thus, there is mounting evidence against current empirical models of Hamilton, Bowles in which attenuation increases with depth in fine-grained sediments. The decreasing attenuation may be a useful clue for development of sediment acoustic models in fine-grained sediments.

Finally, it is recommended that future attenuation studies report frequency-dependent attenuation scaled by one factor of frequency, e.g., in dB/m/kHz. This substantively improves clarity of attenuation data/model results by substantively reducing the dynamic range.

ACKNOWLEDGEMENTS

The authors gratefully acknowledge the financial support of ONR Ocean Acoustics and wish to thank the captain and crew of the R/V Armstrong for their considerable skill and energy. We also thank Preston Wilson and David Knobles, the Chief Scientists for the SBCEX17. We finally wish to express appreciation to John Goff for making available the mudbase two-way travel time data (Figure 12b), to Mae Jiang for making available the Bayesian uncertainties and Jason Chaytor for helpful discussions and comments on the manuscript.

REFERENCES

[1] A.B. Wood and D.E. Weston, The propagation of sound in mud. *Acta Acustica united with Acustica*, *14*(3), 156-162, 1964.

[2] E.L. Hamilton, Compressional wave attenuation in marine sediments, Geophysics, 37,620-646, 1972.

[3] E.L. Hamilton, Geoacoustic modeling of the seafloor, *J. Acoust. Soc. Am.*, **68**, 1313-1340, 1980.

[4] F.A. Bowles, Observations on attenuation and shear-wave velocity in fine-grained, marine sediments. *J. Acoust. Soc. Am.*, 101, 3385-3397, 1997.

[5] S.K. Mitchell and K.C. Focke, New measurements of compressional wave attenuation in deep ocean sediments, *J. Acoust. Soc. Am*., *67*(5), pp.1582-1589, 1980.

[6] C.W. Holland and S.E. Dosso, Mid frequency shallow-water fine-grained sediment attenuation from waveguide reverberation, J. Acoust. Soc. Am., 134, 131-134, 2013.

[7] T.J. Gorgas, R.H. Wilkens, S.S. Fu, L.N. Frazer, M.D. Richardson, K.B. Briggs, and H. Lee, *In-situ* acoustic and laboratory ultrasonic sound speed and attenuation measured in heterogeneous soft seabed sediments: Eel River shelf, California. Marine Geology, 182, 103-119, 2002.

[8] L.N. Frazer, S.S. Fu, and R.H. Wilkens, Seabed sediment attenuation profiles from a movable sub-bottom acoustic vertical array. *J. Acoust. Soc. Am.*, *106*(1), pp.120-130, 1999.

[9] C.W. Holland, C.M. Smith, Z. Lowe, and J. Dorminy, Seabed observations at the New England Mud Patch: reflection and scattering measurements and direct geoacoustic information, IEEE J. Ocean Eng., in press.

[10] P.S. Wilson, D.P. Knobles, and T.A. Nielsen, Guest Editorial: An Overview of the Seabed Characterization Experiment, *IEEE J. Ocean Eng.,* 45, 1-13, 2020.

[11] J.A. Goff, A.H. Reed, G. Gawarkiewicz, P.S. Wilson, and D.P. Knobles, Stratigraphic analysis of a sediment pond within the New England Mud Patch: New constraints from high-resolution chirp acoustic reflection data, *Marine Geology*, 412, 81-94, 2019.

[12] J.D. Chaytor, M.S. Ballard B.J. Buczkowski, J.A. Goff, K.M. Lee, A.H. Reed, and A.A. Boggess, Measurements of geologic characteristics and geophysical properties of sediments from the New England Mud Patch, IEEE J. Ocean Eng., in review.

[13] J. Belcourt, C.W. Holland, S.E. Dosso, and J. Dettmer, Depth-dependent geoacoustic estimates with dispersion from the New England Mud Patch via reflection coefficient inversion, IEEE J. Oceanic Eng.,45, 69-91, 2020, doi 10.1109/JOE.2019.2900115 (March 2019).

[14] M.J. Buckingham, On pore-fluid viscosity and the wave properties of saturated granular materials including marine sediments, J. Acoust. Soc. Am., **122**, 1486–1501, 2007.

[15] C.A. Nittrouer, D.J. DeMaster, S.A. Kuehl, and B.A. McKee, Association of sand with deposits accumulating on continental shelves, in *Shelf Sands and Sandstones* ed. RJ Knight and JR McLean, Can Soc of Petr. Geologists, Memoir II, 17-25, 1986.

[16] M.S. Ballard, K.M. Lee, A.R. McNeese, P.S. Wilson, J.D. Chaytor, J.A. Goff, and A.H. Reed, *In-situ* Measurements of Compressional Wave Speed During Gravity Coring Operations in the New England Mud Patch, *IEEE J. Ocean Eng., 45,26-38, 2020.*

[17] L.M. Brekhovskikh, and O.A. Godin, Acoustics of layered media II: Point sources and bounded beams, Springer, Berlin Heidelberg, 1999, pg 4, Eq(1.1.9).

[18] C.W. Holland, C.M. Smith, J. Belcourt, and S.E. Dosso, Geoacoustic inferences from seabed reflection measurements on the New England Mud Patch. *J. Acoust. Soc. Am.*, *142*, 2590, 2017.

[19] L. Wan, M. Badiey, D.P. Knobles, P.S. Wilson, and J. Goff, Estimates of Low-Frequency Sound Speed and Attenuation in a Surface Mud Layer Using Low-Order Modes, *IEEE J. Ocean Eng.,* 45, 201-211, 2020.

[20] C.W. Holland and J. Dettmer, *In-situ* sediment dispersion estimates in the presence of discrete layers and gradients, *J. Acoust. Soc. Am.*, 133, 50-61, 2013.

[21] J. Dettmer, C.W. Holland, and S.E. Dosso, Trans-dimensional uncertainty estimation for dispersive seabed sediments, Geophysics, 78, WB63-WB76, 2013.

[22] C.W. Holland and G. Muncill, Acoustic Reflection from Quasi-periodic Sedimentary Sequences, J. Acoust. Soc. Am., 94, 1609-1620, 1993.

[23] M.A. Gutierrez, J. Dvorkin, and A. Nur, Textural sorting effect on elastic velocities, Part I: Laboratory observations, rock physics models, and applications to field data, in *SEG Technical Program Expanded Abstracts 2001*,1760-1763, Soc. Expl. Geophys., 2001.

[24] A.D. Pierce, W.L. Siegmann, and E. M. Brown, Characterization of mud sediments using the frequency dependence pf phase velocity and attenuation of compressional waves, *Proc. Meetings Acoust.*, 31 (1), Art. no. 070002, 2017.

[25] M.A. Biot, Generalized Theory of Acoustic Propagation in Porous Dissipative Media, J. Acoust. Soc. Am., 34, 1254-1264, 1962.